(2)

WRDC-TR-89-2149

IMPROVED ANALYTICAL CAPABILITIES FOR FOIL AIR BEARINGS

Dr Erh-Rong Wu
Phyllis M.K. Wu

Mega Research, Inc
29711 Whitley Collins Drive
Rancho Palos Verdes, CA 90274

January 1990

Final Report for Period 15 September 1988 - 15 September 1989

Approved for Public Release; Distribution is Unlimited

AERO PROPULSION LABORATORY
WRIGHT RESEARCH AND DEVELOPMENT CENTER
AIR FORCE SYSTEMS COMMAND
WRIGHT-PATTERSON AIR FORCE BASE, OHIO 45433-6563

NOTICE

When Government drawings, specifications, or other data are used for any purpose other than in connection with a definitely Government-related procurement, the United States Government incurs no responsibility or any obligation whatsoever. The fact that the government may have formulated or in any way supplied the said drawings, specifications, or other data, is not to be regarded by implication, or otherwise in any manner construed, as licensing the holder, or any other person or corporation; or as conveying any rights or permission to manufacture, use, or sell any patented invention that may in any way be related thereto.

This report is releasable to the National Technical Information Service (NTIS). At NTIS, it will be available to the general public, including foreign nations.

This technical report has been reviewed and is approved for publication.

LEON J. DeBROHUN, Project Engineer
Lubrication Branch
Fuels and Lubrication Division
Aero Propulsion and Power Laboratory

HOWARD F. JONES, Chief
Lubrication Branch
Fuels and Lubrication Division
Aero Propulsion and Power Laboratory

FOR THE COMMANDER

LEO S. HAROOTYAN, JR., Assistant Chief
Fuels and Lubrication Division
Aero Propulsion and Power Laboratory

If your address has changed, if you wish to be removed from our mailing list, or if the addressee is no longer employed by your organization please notify WRDC/POSL, WPAFB, OH 45433-6563 to help us maintain a current mailing list.

Copies of this report should not be returned unless return is required by security considerations, contractual obligations, or notice on a specific document.

UNCLASSIFIED
SECURITY CLASSIFICATION OF THIS PAGE

REPORT DOCUMENTATION PAGE

Form Approved OMB No. 0704-0188

1a. REPORT SECURITY CLASSIFICATION: UNCLASSIFIED	1b. RESTRICTIVE MARKINGS
2a. SECURITY CLASSIFICATION AUTHORITY	3. DISTRIBUTION/AVAILABILITY OF REPORT: Approved for public release; distribution is unlimited.
2b. DECLASSIFICATION/DOWNGRADING SCHEDULE	
4. PERFORMING ORGANIZATION REPORT NUMBER(S): SBIR-88-LUB-1	5. MONITORING ORGANIZATION REPORT NUMBER(S): WRDC-TR-89-2149
6a. NAME OF PERFORMING ORGANIZATION: Mega Research, Inc. / 6b. OFFICE SYMBOL (If applicable)	7a. NAME OF MONITORING ORGANIZATION: Aero Propulsion & Power Lab (WRDC/POSL) Wright Research and Development Center
6c. ADDRESS (City, State, and ZIP Code): 29711 Whitley Collins Drive Ranch Palos Verdes CA 90274	7b. ADDRESS (City, State, and ZIP Code): Wright-Patterson AFB OH 45433-6563
8a. NAME OF FUNDING/SPONSORING ORGANIZATION / 8b. OFFICE SYMBOL (If applicable): WRDC/POSL	9. PROCUREMENT INSTRUMENT IDENTIFICATION NUMBER: F33615-88-C-2851
8c. ADDRESS (City, State, and ZIP Code)	10. SOURCE OF FUNDING NUMBERS

PROGRAM ELEMENT NO.	PROJECT NO.	TASK NO	WORK UNIT ACCESSION NO.
65502F	3005	21	25

11. TITLE (Include Security Classification): Improved Analytical Capabilities for Foil Air Bearings

12. PERSONAL AUTHOR(S): Wu, Erh-Rong; Wu, Phyllis M.K.

13a. TYPE OF REPORT	13b. TIME COVERED	14. DATE OF REPORT (Year, Month, Day)	15. PAGE COUNT
Final	FROM 88-9-15 TO 89-9-15	1990 January	38

16. SUPPLEMENTARY NOTATION

17. COSATI CODES			18. SUBJECT TERMS (Continue on reverse if necessary and identify by block number)
FIELD	GROUP	SUB-GROUP	Foil Air Bearing, Three-Dimensional (3D) Navier-Stokes, Reynolds Equation, Fluid Inertia, Thermoelasticity, Turbulence.
Lubrication	Air Brg	Foil Brg	

19. ABSTRACT (Continue on reverse if necessary and identify by block number)

The completion of this Phase I study has presented an advanced analytic tool for predicting the performance of foil bearing and solid-walled bearing as well, operating at speeds wherein the Reynolds number is no longer small and the effects of the fluid inertia, the heat transfer and the turbulent flow become significant. The tool utilizes the 3-D Navier-Stokes approach for the fluid film thermohydrodynamics and the thermoelasticity treatment for the foil deformation. The Navier-Stokes approach is more complicated than the Reynolds equation approach, conventional or modified for the inclusion of inertia or turbulence. Nevertheless, the N-S approach has the capability of investigating the local behaviors of the lubricant and the foil. Especially, the prediction of temperature variation may eventually help explain the hot spots or burned spots which are often observed in a failed bearing. Two computer programs, 3DNSBRGJ (journal) and 3DNSBRGT (thrust) are developed through this Phase I study. The programs are capable for calculating bearing performance characteristics, and the velocity components, the temperature distribution, the foil deflection, the turbulence energy distribution and its dissipation rate.

20. DISTRIBUTION/AVAILABILITY OF ABSTRACT	21. ABSTRACT SECURITY CLASSIFICATION
☒ UNCLASSIFIED/UNLIMITED ☐ SAME AS RPT. ☐ DTIC USERS	UNCLASSIFIED

22a. NAME OF RESPONSIBLE INDIVIDUAL	22b. TELEPHONE (Include Area Code)	22c. OFFICE SYMBOL
Leon J. DeBrohun	(513) 255-6638	WRDC/POSL

DD Form 1473, JUN 86 — Previous editions are obsolete.

SECURITY CLASSIFICATION OF THIS PAGE
UNCLASSIFIED

INTRODUCTION

Foil bearings are intended to operate at high speeds. For high speed bearings, in general, the effects of fluid inertia, turbulent flow and heat transfer become important issues in analyzing bearing performance characteristics. For the foil bearings, the thermoelasticity of the flexible foils adds complications to the analysis of the high speed bearings. A competent advanced analytical tool for the foil bearings should take the above-mentioned issues into consideration.

The conventional Reynolds equation approach, for several decades, has been a prevailing method for hydrodynamic lubrication analysis. The basic assumptions of the Reynolds equation are: (1) The Reynolds number is very small. (2) The flow across the film is insignificant. And, (3) the fluid is isothermal. Apparently, these assumptions become inadequate as the Reynolds number is greater than the order of magnitude of one.

There have been technical papers and reports contributed to the understanding of the turbulent lubrication, the inertial and the thermal effects. For the turbulent fluid film, the mixing-length [1] and the "wall of the law" [2] and [3] are the two most popular approaches. Launder and Leschziner [4] later employed the low Reynolds number k-e turbulence model [5] to treat slider bearings. The k-e model [6-7] has been proved to be more in line with experimental observations than other turbulence models in various flow situations such as flat plate boundary layers, pipe flows and shear flows of jets. Although the k-e model adds two more equations, the turbulence kinetic energy, K, and the dissipation rate of turbulent energy, e, equations to the computation process, it relates the turbulent viscosity to the local turbulent energy transport and provides a better tool to trace the history of the turbulent flow.

In dealing with the fluid inertia, represented by the convective terms in the momentum equations, most of previous studies integrated the momentum equations across the film gap, a process similar to the derivation of the Reynolds equation. Since the velocity profile is not known beforehand in the film gap, to carry out the integration, a velocity profile is assumed or borrowed from the non-inertial solution.

The runner surface and the bearing (or foil) surface are not parallel. The inclination of the surfaces results in a transverse velocity component contributed by the runner's tangential velocity, adding to the flow across the film gap. This transverse velocity component becomes more pronounced as the runner's speed increases. Consequently, an assumed velocity profile may not be able to reveal the local flow behaviour especially for the high speed bearings. The across-film integration, at best, can only catch the velocities at the two ends.

The present study adopts a three dimensional Navier-Stokes approach with the low Reynolds number k-e turbulence model by Jones and Launder [5] for the turbulent flow case. The Navier-Stokes equations are written in cylindrical coordinates so that the curvature effects including the centrifugal and the coriolis accelerations can be taken into account. The momentum equations, the continuity equation, the energy equation, and the k-e equations are solved by the SIMPLE (Semi-Implicit-Pressure-Linked-Equations) algorithm developed by Patankar and Spalding [8] and elaborated in the book by Patankar [9].

The thermohydrodynamic solution of the fluid film provides the pressure and the temperature distributions on the foil surfaces. The fluid pressure and the thermal effect cause the deformation of the foils. To analyze the thermoelasticity of the foil, a thin plate model is chosen to simulate the foil. The governing thermoelasticity equation, a fourth order partial differential equation, is solved by finite-difference approximations. The result of the numerical calculation gives the foil deflection which, in turn, changes the fluid film shape.

The interaction between the thermohydrodynamics of the fluid film and the thermoelasticity of the foil is dealt with by combining the two parts of computations and performing iterations to reach a convergent solution.

For the Phase I study, two computer programs are developed, the journal bearing and the thrust bearing programs. The two kinds of bearings have quite different geometries. Therefore, the equations for the two bearings are not the same. These two programs can be used to analyze the steady-state performances of the two kinds of bearings, including the effects of the inertia, the heat transfer and the turbulent flow. The programs can be utilized for the foil bearing as well as the solid-walled bearing analysis. The latter is simply a special case as far as the program capability is concerned.

Computational examples are presented for both the thrust and the journal bearings. The performance characteristics, such as the load carrying capacity, the frictional coefficient and the attitude angle (for the journal bearing) are calculated. Results are compared with available solid-walled bearing data, [10] and [11] to verify the accuracy and to reveal the inertial, the thermal and the turbulent flow effects.

The Navier-Stokes approach differs from the Reynolds equation approach not only in solving more complicated differential equations and realizing the above-mentioned three effects, but also in providing an advanced tool for visualizing how the fluid enter the bearing and how the flow behaves locally. The continuation of this study such as a Phase II study should focus on the trasient case and the combination of the fluid dynamics and the rotor dynamics. Hence, a better picture of the dynamic behaviors of the rotor-bearing can be obtained. with limited time and budget, the Phase I study has achieved the goal of establishing the fundation for pursuing further studies.

ANALYSIS

Basically, the fluid film in either a journal bearing or a thrust bearing is equivalent to the flow between two inclined surfaces. For the journal bearing, the flow is between two eccentric cylinders, while for the thrust bearing, it is between two unparallel disks. To describe the three dimensional flow behaviors and to consider the curvature effects including the centrifugal and the coroilis forces, cynlindrical coordinates are chosen to derive the governing equations. The main geometrical difference between the journal bearing and the thrust bearing lies in the direction of the film gap; for the former, the film gap is in the radial (r) direction, while for the latter, it is in the axial (z) direction. Nevertheless, both bearings have a common feature that is a main flow in the circumferential (Θ) direction. Due to this dominating flow, the parabolization concept can be applied to the Navier-Stokes equations and the so-called marching technique can be employed in the numerical computation.

Additionally, because of the eccentricity of the cylinders, in the journal bearing case, and the unparallelness of the disks, in the thrust bearing case, the main flow, V_θ, has components in the other two directions, i.e., the r and z directions. Furthermore, the shaft misalignment, if present in the journal bearing, and the foil deflection will modify fluxes contributed by V_θ to the r and z directions. Consequently, film-shape fitted coordinates transformations are very much desired to enable the realization of these additional fluxes in both the r and z directions.

In the following, formulations, coordinate transformations and numerical solution procedures will be elaborated:

A. FORMULATIONS

The Navier-Stokes equations for the compressible flow can be written as

$$\rho \frac{dU}{dt} = \rho g - \nabla p + \mu \nabla^2 U + \frac{1}{3} \mu \nabla (\nabla \cdot U) \qquad (1)$$

The continuity equation in the cylindrical coordinates takes the form

$$\frac{\partial \rho}{\partial t} + \frac{1}{r} \frac{\partial}{\partial r} (\rho r V_r) + \frac{1}{r} \frac{\partial}{\partial \theta} (\rho V_\theta) + \frac{\partial}{\partial z} (\rho V_z) = 0 \qquad (2)$$

The energy equation in terms of the temperature, T, can be written as

$$\rho c_p \left[\frac{\partial T}{\partial t} + U \cdot \nabla T \right] = \frac{\partial p}{\partial t} + U \cdot \nabla p + k \nabla^2 T + \phi \qquad (3)$$

where k is the thermal conductivity and ϕ is the dissipation function which can be expressed as

$$\phi = (\phi' \cdot \nabla) \cdot U \qquad (4)$$

where ϕ' is the stess matrix defined as

$$\phi' = \begin{pmatrix} \sigma_{rr} & \tau_{r\theta} & \tau_{rz} \\ \tau_{\theta r} & \sigma_{\theta\theta} & \tau_{\theta z} \\ \tau_{zr} & \tau_{z\theta} & \sigma_{zz} \end{pmatrix} \qquad (5)$$

So far, the above equations describe the thermohydrodynamic behaviors of the fluid film. For the turbulent flow, in the high speed bearing case, the turbulence disturbance components are governed by the Reynolds stress equation:

$$\frac{D\overline{u_i u_j}}{Dt} = - \frac{\partial}{\partial x_k} (\overline{u_i u_j u_k}) + \delta_{ik} \frac{\overline{u_i p'}}{\rho} + \delta_{jk} \frac{\overline{u_j p'}}{\rho} - \nu_t \frac{\partial \overline{u_i u_j}}{\partial x_k})$$
$$+ \frac{\overline{p'}}{\rho} \left(\frac{\partial u_i}{\partial x_j} + \frac{\partial u_j}{\partial x_i} \right) - (\overline{u_i u_k} \frac{\partial U_j}{\partial x_k} + \overline{u_j u_k} \frac{\partial U_i}{\partial x_k}) - 2\nu_t \frac{\overline{\partial u_i}}{\partial x_k} \frac{\partial u_j}{\partial x_k} \qquad (6)$$

where i,j,k denote the three orthogonal coordinate directions, and U is the mean flow vector.

It is prohibitive to solve equation (5), even numerically. Several turbulence models have been developed to define the turbulent viscosity. The k-e model is the most popular and well tested model in the current stage of the computational fluid dynamics.

K is the turbulent kinetic energy and e is the rate of the turbulent energy dissipation. They are defined as

$$k = \frac{1}{2}\overline{u_i u_i} \quad , \text{ and } \quad e = \nu_t \overline{\frac{\partial u_i}{\partial x_k}\frac{\partial u_i}{\partial x_k}} \tag{7}$$

The turbulent viscosity is then defined as

$$\mu_t = C_\mu \rho K^2 / e \tag{8}$$

Based on Launder and Leschziner's simplification, the k-e equations for the low Reynolds number case which is suitable for the fluid film in lubrication can be expressed as

$$\frac{\partial}{\partial z}\left[\left(\mu + \frac{\mu_t}{\sigma_k}\right)\frac{\partial K}{\partial z}\right] + \mu_t\left[\left(\frac{\partial V_r}{\partial z}\right)^2 + \left(\frac{\partial V_\theta}{\partial z}\right)^2\right]\rho e - 2\mu\left(\frac{d\sqrt{K}}{dz}\right)^2 = 0 \tag{9}$$

$$\frac{\partial}{\partial z}\left[\left(\mu + \frac{\mu_t}{\sigma_e}\right)\frac{\partial e}{\partial z}\right] + C_1\frac{e}{K}\mu_t\left[\left(\frac{\partial V_r}{\partial z}\right)^2 + \left(\frac{\partial V_\theta}{\partial z}\right)^2\right] - C_2\rho\frac{e^2}{K} + C_3\frac{\mu\mu_t}{\rho}\left[\left(\frac{\partial V_r}{\partial z}\right)^2 + \left(\frac{\partial V_\theta}{\partial z}\right)^2\right] = 0 \tag{10}$$

Here, it should be noted that the z-direction is the direction across the film gap; for this case, it applys to a thrust bearing.

In the equations (9) and (10), μ , σ_k, σ_e are the laminar viscosity and the Prandtal numbers for k and e. C_μ, C_1, C_2 and C_3 are defined as follows:

$C_1 = 1.44$, $C_2 = 1.92\ [\ 1 - 0.3 \exp(-Re_t^2)\ ]$

$C_3 = 2.0$, $\sigma_k = 1.0$, $\sigma_e = 1.3$

$C_\mu = 0.09 \exp[\ -3.4/(\ 1 + Re/50\ )\ ]$

$Re_t = \rho k^2 / \mu e$

Re_t is the turbulent Reynolds number.

Considering the steady state case (neglecting $\frac{\partial}{\partial t}$ terms), applying the parabolization concept (neglecting the 2nd order derivatives with respect tc θ, i.e., $\frac{\partial^2}{\partial \theta^2}$) and utilizing the continuity equation, all the above-mentioned governing equations, including three momentum equations, two turbulence equations (k-e) and one energy (temperature) equation, can be written in a generalized form:

$$\frac{1}{r}\frac{\partial}{\partial r}(r\rho V_r \phi) + \frac{1}{r}\frac{\partial}{\partial \theta}(\rho V_\theta \phi) + \frac{\partial}{\partial z}(\rho V_z \phi)$$

[convection terms]

$$= \frac{1}{r}\frac{\partial}{\partial r}\left(r\Gamma_\phi \frac{\partial \phi}{\partial r}\right) + \frac{1}{r}\frac{\partial}{\partial z}\left(r\Gamma_\phi \frac{\partial \phi}{\partial z}\right) + S_\phi \qquad (11)$$

[diffusion terms] [source terms]

ϕ symbolizes the six dependent variables. Γ_ϕ is the effective viscosity; $\Gamma_\phi = \mu + \frac{\mu_t}{\sigma_t}$. S_ϕ represents the source terms.

The convection terms, left hand side of the equation (11) and the diffusion terms, except Γ_ϕ, are standard for all ϕ's. The Γ_ϕ and S_ϕ for all ϕ's are tabulated in Table 1.

ϕ	Γ_ϕ	S_ϕ
V_r	$\mu + \frac{\mu_t}{\sigma_t}$ (μ_{eff})	$-\frac{\partial p}{\partial r} + \rho\frac{V_\theta^2}{r} - \frac{\Gamma_\phi}{3}\left(\frac{4V_r}{r^2} + \frac{7}{r^2}\frac{\partial V_\theta}{\partial \theta}\right)$
V_θ	μ_{eff}	$-\frac{1}{r}\frac{\partial p}{\partial \theta} - \rho\frac{V_r V_\theta}{r} + \Gamma_\phi\left(\frac{7}{3}\frac{1}{r^2}\frac{\partial V_r}{\partial \theta} - \frac{V_\theta}{r^2}\right)$
V_z	μ_{eff}	$-\frac{\partial p}{\partial z} + \frac{\Gamma_\phi}{3}\frac{\partial^2 V_z}{\partial z^2}$
T	$\frac{\mu}{\sigma} + \frac{\mu_t}{\sigma_t}$	$\frac{1}{C_p}\{\frac{1}{r}\frac{\partial}{\partial r}(rV_r p) + \frac{1}{r}\frac{\partial}{\partial \theta}(V_\theta p) + \frac{\partial}{\partial z}(V_z p) + \Gamma_\phi[(\frac{\partial V_\theta}{\partial z})^2 + (\frac{\partial V_\theta}{\partial r})^2 + (\frac{V_\theta}{r})^2]\}$
K	$\mu + \frac{\mu_t}{\sigma_k}$	$\mu_t[(\frac{\partial V_r}{\partial z})^2 + (\frac{\partial V_\theta}{\partial z})^2] - \rho e - 2\mu(\frac{d\sqrt{K}}{dz})^2$
e	$\mu + \frac{\mu_t}{\sigma_e}$	$C_1\frac{e}{K}\mu_t[(\frac{\partial V_r}{\partial z})^2 + (\frac{\partial V_\theta}{\partial z})^2] - C_2\rho\frac{e^2}{K} + C_3\frac{\mu\mu_t}{\rho}[(\frac{\partial^2 V_r}{\partial z^2})^2 - (\frac{\partial^2 V_\theta}{\partial z^2})^2]$

Table I

Table I is applicable to the thrust bearing. For the journal bearing, the roles of r and z are exchanged. Terms of Table I can be modified accordingly to suit the journal bearing case.

The next region to be considered is the foil which will deform under the influence of the fluid film pressure and the thermal effect. The equation describing the thermoelastic behavior of the foil which is modelled as a thin plate, is adopted from Parkus' book [12]:

$$\frac{E t^3}{12(1-\nu^2)} \nabla^4 w = p - (1+\nu) \frac{E t^3}{12(1-\nu^2)} \alpha \nabla^2 m_T \qquad (12)$$

In writing the equation (12), the deflection caused by membrane forces has been neglected. This is based on the assumption that the deflection due to stretching is small in comparison with bending. In the equation (12), the meanings of symbols are:

w : deflection in the direction normal to the foil surface

E : Young's modulus

ν : Poisson's ratio

t : foil thickness

α : thermal expansion coefficient

p : fluid film pressure

m_T : thermal moment; it is defined as

$$m_T = \frac{12}{t^3} \int_{-t/2}^{t/2} T z \, dz \qquad (13)$$

The factor $\frac{E t^3}{12(1-\nu^2)}$ is the so-called bending stiffness. Let

$$\bar{K} = \frac{E t^3}{12(1-\nu^2)}$$

For bearings with combined top and bottom foils (Fig.1) such as MTI's journal and thrust bearings, and AiResearch's thrust bearing, an equivalent bending stiffness can be derived as follows:

$$\bar{K}_t = \frac{E t_1^3}{12(1-\nu^2)}$$

$$\bar{K}_B = \frac{E t_2^3}{2(1-\nu^2)\ell_o^3} \quad \text{(referred to [13] \& [14])}$$

and, $$\bar{K}_{eq} = \frac{\bar{K}_t \bar{K}_B}{\bar{K}_t + \bar{K}_B} \qquad (14)$$

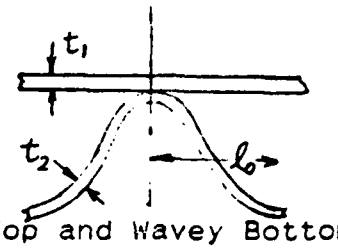

Fig.1 Top and Wavey Bottom Foils

To combine the equation (12) with the equation (13), we take a simplified model considering one dimensional heat conduction across the foil thickness with boundary conditions depicted in Fig. 2.

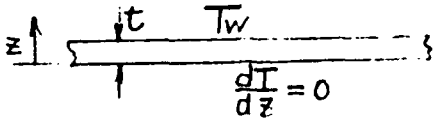

Fig. 2 Heat Conduction across the Foil

Consequently, the temperature distribution across the foil thickness, in terms of the wall temperature, Tw, is:

$$T = T_w \left(\hat{z} + \frac{1}{2} \right)^2 \qquad (15)$$

$$\hat{z} = \frac{z}{t}$$

Substituting the equation (15) into the equation (13), we obtain

$$m_T = \frac{12t^2}{t^3} \int_{-1/2}^{1/2} T_w \left(\hat{Z} + \frac{1}{2}\right)^2 \hat{Z}\, d\hat{Z}$$

$$= \frac{T_w}{t} \qquad (16)$$

Using the equation (16), the thermoelasticity equation (12) becomes

$$\bar{K} \nabla^4 W = p - \frac{\bar{K}(1+\nu)\alpha}{t} T_w \qquad (17)$$

For the journal bearing, p and Tw are functions of θ and z while for the thrust bearing they are functions of r and θ.

B. Coordinate Transformations

As mentioned previously, due to the film thickness variation, the main flow contributes fluxes to the other two directions. Since the film gap direction of the journal bearing differs from that of the thrust bearing, different coordinate transformations should be selected for the two bearings.

For the thrust bearing, we choose the following transformations of coordinates (referred to the sketch shown in Fig. 3):

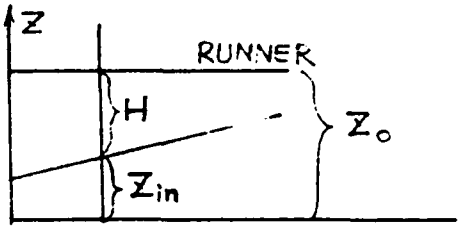

Fig.3 Coordinate Transformations (Thrust Bearing)

$$\hat{r} = \frac{r - r_{in}}{\Delta R}$$

$$\hat{\theta} = \frac{\theta - \theta_{in}}{\Theta} \qquad (18)$$

$$\hat{z} = \frac{z - z_{in}}{H} = \frac{z - (z_c - H)}{H} = \frac{z - z_c}{H} + 1$$

where $\Delta R = r_{out} - r_{in}$, the difference between the outer radius and the inner radius. Θ is the pad angle and H is the local film thickness. The new coordinates represent a set of canonical forms which define each variable in a unit range, i.e., 0 to 1. Applying the chain rule of differentiation, we have

$$\frac{\partial}{\partial r} = \frac{\partial}{\partial \hat{r}}\frac{\partial \hat{r}}{\partial r} + \frac{\partial}{\partial \hat{\theta}}\frac{\partial \hat{\theta}}{\partial r} + \frac{\partial}{\partial \hat{z}}\frac{\partial \hat{z}}{\partial r} = \frac{1}{\Delta R}\frac{\partial}{\partial \hat{r}} + \frac{(1-\hat{z})}{H}\frac{\partial H}{\partial r}\frac{\partial}{\partial \hat{z}}$$

$$\frac{\partial}{\partial \theta} = \frac{\partial}{\partial \hat{r}}\frac{\partial \hat{r}}{\partial \theta} + \frac{\partial}{\partial \hat{\theta}}\frac{\partial \hat{\theta}}{\partial \theta} + \frac{\partial}{\partial \hat{z}}\frac{\partial \hat{z}}{\partial \theta} = \frac{1}{\Theta}\frac{\partial}{\partial \hat{\theta}} + \frac{(1-\hat{z})}{H}\frac{\partial H}{\partial \theta}\frac{\partial}{\partial \hat{z}} \qquad (19)$$

$$\frac{\partial}{\partial z} = \frac{\partial}{\partial \hat{r}}\frac{\partial \hat{r}}{\partial z} + \frac{\partial}{\partial \hat{\theta}}\frac{\partial \hat{\theta}}{\partial z} + \frac{\partial}{\partial \hat{z}}\frac{\partial \hat{z}}{\partial z} = \frac{1}{H}\frac{\partial}{\partial \hat{z}}$$

Substitution of the coordinate transformations represented by the equation (19) into the general transport equation (11) results in

$$\frac{1}{r}\left[\frac{1}{\Delta R}\frac{\partial}{\partial \hat{r}}(r\rho V_r \phi)\right] + \frac{1}{r\Theta}\frac{\partial}{\partial \hat{\theta}}(\rho V_\theta \phi)$$

$$-\frac{\partial}{\partial \hat{z}}\left[\rho\left(V_z + \frac{(1-\hat{z})}{H}\frac{\partial H}{\partial r}V_r + \frac{(1-\hat{z})}{H}\frac{\partial H}{\partial \theta}V_\theta\right)\phi\right]$$

$$= \frac{1}{r}\frac{1}{(\Delta R)^2}\frac{\partial}{\partial \hat{r}}\left(r\Gamma_\phi \frac{\partial \phi}{\partial \hat{r}}\right) + \frac{1}{H^2}\left\{\frac{\partial}{\partial \hat{z}}\left[1 + (1-\hat{z})^2\left(\frac{\partial H}{\partial r}\right)^2\right]\Gamma_\phi \frac{\partial \phi}{\partial \hat{z}}\right\} + S_\phi \qquad (20)$$

For the journal bearing, the film gap is in the radial direction. Therefore, referring to Fig. 4, we select the coordinate transformations of the following forms:

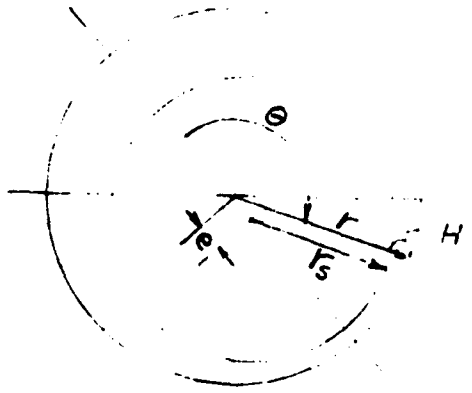

Fig. 4 Coordinate Transformations
of Journal Bearing

$$\hat{r} = \frac{r - r_s + e\cos\theta}{H} \qquad (H = C + e\cos\theta)$$

where r_s is the radius of the shaft;
C is the radial clearance;
e is the eccentrical displacement of the shaft from the bearing center.

$$\hat{\theta} = \frac{\theta - \theta_{in}}{\Theta}$$

$$\hat{z} = \frac{z - z_{in}}{L} \qquad L : \text{bearing length} \tag{21}$$

The chain rule of differentiation yields:

$$\frac{\partial}{\partial r} = \frac{1}{H}\frac{\partial}{\partial \hat{r}}$$

$$\frac{\partial}{\partial \theta} = \frac{1}{\Theta}\frac{\partial}{\partial \hat{\theta}} + \frac{(1-\hat{r})}{H}\frac{\partial H}{\partial \theta}\frac{\partial}{\partial \hat{r}} \tag{22}$$

$$\frac{\partial}{\partial z} = \frac{1}{L}\frac{\partial}{\partial \hat{z}} + \frac{(1-\hat{r})}{H}\frac{\partial H}{\partial z}\frac{\partial}{\partial \hat{r}}$$

With the replacement of the equation (22) for the equation (19), the general transport equation becomes:

$$\frac{1}{r}\left\{\frac{1}{H}\frac{\partial}{\partial \hat{r}}\left[r\rho\phi\left(V_r + \frac{(1-\hat{r})}{1}\frac{\partial H}{\partial \theta}V_\theta + \frac{(1-\hat{r})}{1}\frac{\partial H}{\partial \hat{z}}V_{\hat{z}}\right)\right]\right\}$$
$$-\frac{1}{r\Theta}\frac{\partial}{\partial \theta}(\rho V_\theta \phi) + \frac{1}{L}\frac{\partial}{\partial \hat{z}}(\rho V_{\hat{z}}\phi)$$
$$= \frac{1}{r}\frac{1}{H^2}\frac{\partial}{\partial \hat{r}}\left\{r\Gamma_\phi\left[1 + (1-\hat{r})^2\left(\frac{\partial H}{\partial \hat{z}}\right)^2\right]\frac{\partial \phi}{\partial \hat{r}}\right\} + \frac{1}{L^2}\frac{\partial}{\partial \hat{z}}\left(\Gamma_\phi \frac{\partial \phi}{\partial \hat{z}}\right)$$
$$+ S_\phi \qquad (23)$$

In the equations (20) and (23), those terms representing the film thickness variation, namely, $\frac{\partial H}{\partial r}$ and $\frac{\partial H}{\partial \theta}$ in (20), and $\frac{\partial H}{\partial \theta}$ and $\frac{\partial H}{\partial \hat{z}}$ in (23), confirm the fact that the flow in the circumferential and axial directions, (or circumferential and radial directions) contribute flux components to the flow across the film gap. For high speed bearings, the flux component contributed by, especially, the circumferential flow becomes pronounced. The two dimensional approach or the Reynolds equation approach may not be able to reveal locally the significance of this transverse flux increase.

The steady-state continuity equation, for the thrust bearing, becomes

$$\frac{1}{r}\frac{1}{\Delta R}\frac{\partial}{\partial \hat{r}}(\rho r V_r) + \frac{1}{r\theta}\frac{\partial}{\partial \theta}(\rho V_\theta)$$
$$+ \frac{\partial}{\partial \hat{z}}\left[\rho\left(V_{\hat{z}} + \frac{1-\hat{z}}{H}\frac{\partial H}{\partial \theta}V_\theta + \frac{1-\hat{z}}{H}\frac{\partial H}{\partial r}V_r\right)\right] = 0 \qquad (24)$$

For the journal bearing, the continuity equation takes the form:

$$\frac{1}{r\Theta}\frac{\partial}{\partial \theta}(\rho V_\theta) + \frac{1}{L}\frac{\partial}{\partial \hat{z}}(\rho V_{\hat{z}})$$
$$- \frac{1}{r}\frac{1}{H}\frac{\partial}{\partial \hat{r}}\left\{\rho r\left[V_r - \frac{(1-\hat{r})}{r}\frac{\partial H}{\partial \theta}V_\theta + (1-\hat{r})\frac{\partial H}{\partial \hat{z}}V_{\hat{z}}\right]\right\} = 0 \qquad (25)$$

C. Numerical Solution Procedures

(I) Finite Difference Equations

The geometry and coordinates of the journal bearing will be used to illustrate the construction of finite difference equations.

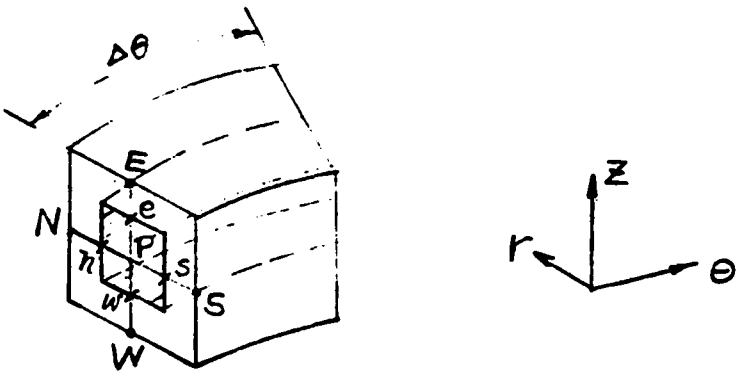

Fig. 5 Control Volume and Grid System

The numerical computation will be carried out step by step, the so-called marching process, in the circumferential (θ) direction. The range of θ, such as the arc angle of a partial arc journal bearing, is divided into a finite number of steps. At each step, the r-z plane is discretized into a grid network. Fig. 5 shows a central point P surrounded bye four points denoted as W (west), E (east), S (south) and N (north). Then, a control volume is constructed by selecting the middle grid points, the lower case w,e,s and n, on the r-z plane, and a depth Δθ. The shaded area in Fig. 5 indicates one of the control volume surfaces on the r-z plane.

The general transport equation and the continuity equation are integrated over the control volume to obtain the finite-difference equations. The transport equation represents a convection-diffusion problem.

In computational fluid dynamics (CFD), it is well known that the commonly used central-difference scheme will lead to unstable solutions as the convection is much stronger than the diffusion. To prevent numerical instability, the upwind difference scheme will be used.

To simplify the expression of the transport equation, we define the following symbols:

$$
\begin{aligned}
F_1 &= \rho V_z \\
F_2 &= \rho V_\theta \\
F_3 &= \rho V_r + \frac{(1-\hat{r})}{r}\left(\frac{\partial H}{\partial \theta}\right)\rho V_\theta + (1-\hat{r})\frac{\partial H}{\partial z}\rho V_z \\
D_1 &= \Gamma_\phi \\
D_2 &= \{1 + [(1-\hat{r})\frac{\partial H}{\partial z}]^2\}\Gamma_\phi \\
A_r &= Lr\Theta\,(\hat{\theta}_2 - \hat{\theta}_1)\,(\hat{z}_e - \hat{z}_w) \\
A_\theta &= LH\,(\hat{r}_n - \hat{r}_s)\,(\hat{z}_e - \hat{z}_w) \\
A_z &= \frac{1}{2}\,G\,H^2\,(\hat{r}_n^2 - \hat{r}_s^2)\,(\hat{\theta}_2 - \hat{\theta}_1)
\end{aligned}
\qquad (26)
$$

Furthermore, subscripts n,s,e,w and up are used to indicate five locations; up is the up-stream plane, i.e., $\hat{\xi}_1$ plane.

The upwind difference scheme can be expressed as

$$(F_1\phi)_e = \phi_P \| F_{1e}, 0 \| - \phi_E \| -F_{1e}, 0 \| \qquad (27)$$

where $\| a, b \|$ = maximum of (a,b)

If $F_{1e} > 0$, then $(F_1\phi)_e = F_{1e}\phi_P$
If $F_{1e} < 0$, then $(F_1\phi)_e = F_{1e}\phi_E$

Using the above-defined symbols, the transport equation becomes

$$a_P \phi_P = a_E \phi_E + a_N \phi_N + a_W \phi_W + a_S \phi_S - Sc\phi + F_{2up} \phi_{up} A_\theta \qquad (28)$$

where

$$a_E = \{ 0 \quad -F_{1e}, \quad 0 \quad] + \frac{D_{1e}}{[\Delta \hat{z}_e} \} A_{ze}$$

$$a_W = \{ 0 \quad F_{1w}, \quad 0 \quad] + \frac{D_{1w}}{[\Delta \hat{z}_w} \} A_{zw}$$

$$a_N = \{ 0 \quad -F_{3n}, \quad 0 \quad] + \frac{D_{2n}}{H[\Delta \hat{r}_n} \} A_{rn} \qquad (29)$$

$$a_S = \{ 0 \quad F_{3s}, \quad 0 \quad] + \frac{D_{2s}}{H[\Delta \hat{r}_s} \} A_{rs}$$

$$a_P = a_E + a_W + a_N + a_S + (F_{1e} - F_{1w}) + (F_{3n} - F_{3s}) + S_{P,\phi}$$

The source term has been split into two parts:

$$S_\phi = S_{C,\phi} - S_{P,\phi} \phi_P \qquad (30)$$

The continuity equation becomes

$$(F_{3n} A_{rn} - F_{3s} A_{rs}) + (F_{1e} A_{ze} - F_{1w} A_{zw})$$

$$- (F_{2,dn} A_{\theta_2} - F_{2,up} A_{\theta_1}) = 0 \qquad (31)$$

Finite difference equations for the thermoelasticity equation (17) are to be constructed on the r-$\hat{e}$ plane for the thrust bearing and on the z-$\hat{e}$ plane for the journal bearing. Here, we take the journal bearing case as an illustration example. The same derivation procedures are applicable to the thrust bearing case.

We set up grid network on the bearing foil and select eight grid points surrounding the central point P. The governing equation has bi-harmonic functions; it needs 9 points to approximate the fourth derivatives with the use of central-differencing scheme which is suitabel for this case.

Referring to the grid system shown in Fig. 6, the thermoelasticity equation becomes

$$a_P w_P = a_{NN} w_{NN} + a_N w_N + a_{SS} w_{SS} + a_S w_S + a_{EE} w_{EE} + a_E w_E + a_{WW} w_{WW} + a_W w_W + S \qquad (32)$$

where

$$a_{NN} = \frac{1}{(r_p \Delta\theta)^4} \qquad a_{SS} = a_{NN}$$

$$a_N = \frac{-4}{(r_p \Delta\theta)^4} \qquad a_S = a_N$$

$$a_{EE} = \frac{1}{(\Delta z)^4} \qquad a_{WW} = a_{EE}$$

$$a_E = \frac{-4}{(\Delta z)^4} \qquad a_W = a_E$$

$$a_P = a_{NN} + a_N + a_{SS} + a_S + a_{EE} + a_E + a_{WW} + a_W$$

$$S = \frac{p_p}{k} - \frac{(1+\nu)\alpha}{t}\left\{\frac{T_E - 2T_P + T_W}{(\Delta z)^2} + \frac{T_N - 2T_P + T_S}{(r_p \Delta\theta)^2}\right\}$$

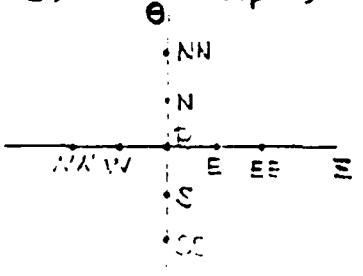

Fig. 6 Grid System for Thermoelasticity Eq.

D. Procedures of SIMPLE Algorithm

The transport and continuity equations are to be solved by the SIMPLE algorithm described in Patankar's book [9]. The word SIMPLE stands for Semi-Implicit Method for Pressure-Linked Equations.

The major operations of the SIMPLE algorithm can be summarized as

(1) Guess the pressure field denoted as p*.

(2) Solve the momentum equations to obtain V_r^* , V_θ^* and V_z^*.

(3) Solve the pressure-correction equation to obtain p'.

(4) Revise the pressure p by adding p' to p*.

(5) Correct the velocity components by using p'.

(6) Solve the transport eqution for other ϕ's such as temperature, T k and e.

Referring to the finite difference equation (28), the momentum equations can be written as

$$V_{\theta p} = \sum \bar{A}_i V_{\theta i} + Sc_\theta + (p_u - p_p) D_p^\theta$$

$$V_{rp} = \sum \bar{A}_i V_{ri} + Sc_r + (p_s - p_p) D_p^r$$

$$V_{zp} = \sum \bar{A}_i V_{zi} + Sc_z + (p_w - p_p) D_p^z$$

where

$$D_p^\theta = \frac{A_\theta}{(a_p^\theta + S_{p\theta})}, \quad D_p^r = \frac{A_r}{(a_p^r + S_{pr})} \quad \text{and} \quad D_p^z = \frac{A_z}{(a_p^z + S_{pz})}$$

Let

$$
\begin{aligned}
p &= p^* + p' \\
V_\theta &= V_\theta^* + V_\theta' \\
V_r &= V_r^* + V_r' \\
V_z &= V_z^* + V_z'
\end{aligned}
\qquad (34)
$$

The primed terms p', V_θ', V_r' and V_z' are correction terms.

Substitution of the equation (34) into the equation (33) results in

$$
\begin{aligned}
V_\theta' &= \sum \bar{A}_i V_{\theta i}' + (p_u' - p_d') D_p^\theta \approx (p_u' - p_d') D_p^\theta \\
V_r' &= \sum \bar{A}_i V_{ri}' + (p_s' - p_p') D_p^r \approx (p_s' - p_p') D_p^r \\
V_z' &= \sum \bar{A}_i V_{zi}' + (p_w' - p_p') D_p^z \approx (p_w' - p_p') D_p^z
\end{aligned}
\qquad (35)
$$

The drop of the terms of $\sum \bar{A}_i V_{\phi i}'$ accounts for the name of Semi-Implicit method. Since the equation (35) has to satisfy the continuity equation and the above-mentioned operations are to be iterated until a converged solution is reached, the Semi-Implicit process will not sacrifice the accuracy of the calculation.

Substitution of the equation (35) into the continuity equation (31) results in a pressure correction equation which has the following form:

$$
a_p' \; p_p' = a_E' \; p_E' + a_W' \; p_W' + a_N' \; p_N' + a_S' \; p_S' + b + a_u' \; p_u' \qquad (36)
$$

where

$$
a_E' = \rho_e D_e^z A_{ze}
$$

$$
a_W' = \rho_w D_w^z A_{zw}
$$

$$a'_N = (D_n^r + B_{2n} D_n^\theta + B_{1n} D_n^z) A_{rn} \rho_n$$

$$a'_S = (D_S^r + B_{2S} D_S^\theta + B_{1S} D_S^z) A_{rS} \rho_S$$

$$a'_u = \rho_u D_u^\theta A_{\theta u}$$

$$a'_P = a'_E + a'_W + a'_N + a'_S + a'_u$$

$$B_1 = (1-\hat{r}) \frac{\partial H}{\partial z} \quad , \quad B_2 = \frac{(1-\hat{r})}{r} \frac{\partial H}{\partial \theta}$$

and,

$$b = \rho_n A_{rn} (V_{rn}^* + B_{2n} V_{\theta n}^* + B_{1n} V_{zn}^*) - \rho_S A_{rS} (V_{rS}^* + B_{2S} V_{\theta S}^* + B_{1S} V_{zS}^*)$$
$$+ \rho_d V_{\theta d}^* A_{\theta d} - \rho_u V_{\theta u}^* A_{\theta u} + \rho_e V_{ze}^* A_{ze} - \rho_w V_{zw}^* A_{zw}$$

With the establishment of the quations (34) and (36), the SIMPLE algorithm procedures can be readily carried out. The only step left out is the iteration process. For the present case, either the journal bearing or the thrust bearing, the dominant flow is in the circumferential (Θ) direction; especially, in the journal bearing, the flow is in cyclical pattern. Consequently, the numerical calculation is marched in the Θ direction and iterated in Θ until a converged solution is obtained.

The solutions of the transport equation provide the pressure and the temperature distributions on the foil surface. Therefore, the numerical calculation of the thermoelasticity equation (32) can be solved by any algebraic equation solver. The Gauss-Seidel (with over-relaxation) iteration is employed to carry out the calculation of the foil deflection.

The foil deflection changes the fluid film shape, which in turn affects the momentum and the temperature fields in the fluid film. This fluid-foil interaction has to be iterated to reach a converged status with a constraint such as that the supporting load is equal to the shaft weight or the frictional force is equal to a required value.

RESULTS AND DISCUSSION

Load capacity (dimensional and dimensionless), friction force (dimensional and dimensionless) and attitude angle (for the journal bearing) are calculated as follows:

(I) Journal Bearing

$$W_1 = W \sin\phi = \int_0^{\ell}\int_0^{2\pi}(p_w - p_a)(\sin\theta)\, r_s\, d\theta\, dz$$

$$W_2 = W \cos\phi = \int_0^{\ell}\int_0^{2\pi}(p_w - p_a)(\cos\theta)\, r_s\, d\theta\, dz$$

where W is the dimensional load capacity;
p_w is the pressure distribution on the shaft surface;
p_a is the ambient pressure;
ℓ is the length of the shaft.

Hence,

$$W = \sqrt{W_1^2 + W_2^2}$$

The attitude angle is

$$\phi = \tan^{-1}\left(\frac{W_1}{W_2}\right)$$

The dimensionless load capacity is defined (to be compatible with the definition given in [11]) as:

$$\bar{W} = \frac{W}{p_a \ell D}$$

The friction forces are :

$$F_s = \int_0^{\ell}\int_0^{2\pi} \tau_{ws}\, r_s\, d\theta\, dz \qquad \text{(on the shaft surface)}$$

$$F_b = \int_0^{\ell}\int_0^{2\pi} \tau_{wb}\, r_b\, d\theta\, dz \qquad \text{(on the bearing surface)}$$

where τ_{ws} is the shear stress on the shaft surface while τ_{wb} is the shear stress on the bearing (foil) surface.
The dimensionless friction coefficient is defined (referred to [11]) as:

$$\eta = \frac{F_s}{p_a \ell D W}\left(\frac{r_s}{C}\right)$$

(II) Thrust Bearing

The load capacity is calculated by integrating the pressure over the area of the pad.

$$W_1 = \int_{R_1}^{R_2}\int_0^{\beta}(p_w - p_a)\, r\, d\theta\, dz$$

The total load capacity is the summation of the loads on all pads.

$$W = N(pad)*W_1$$

Dimensionless load capacity is defined (referred to [10]) as:

$$\bar{W} = \frac{6}{\Lambda}\frac{W}{p_a L B}$$

where $B = R_2 - R_1$ and $L = \beta *(R_2 + R_1)/2$.

The friction force is calculated by integrating the shear stress on the bearing surface over the area of the pad.

$$F = \int_{R_1}^{R_2}\int_0^{\beta}\tau_w r\, dr\, d\theta$$

The dimensionless friction coefficient is defined as:

$$\bar{F} = \frac{6F}{p_a \Lambda l H_2}$$

where Λ is the compressbility number and H_2 is the minimum film gap.

Computations of numerical examples are carried out. The results of the computations are presented in the following:

(A) Journal Bearing

For the journal bearing, we consider a bearing and a shafte with the input data:

RS(shaft radius)= 0.0254 meter
RB(bearing radius)= 0.02542673 m
RPM= 50000.0
ALEN(bearing lenght)= 0.0508 m
PAMB(ambient pressure)= 101353.0 newton/sq. m
HC(radial clearance)= 0.000026726 m
EE(radial displacement)= 0.000015036 m

BETA(arc angle)= 6.2832 rad. (full journal bearing)
ALMULAM(laminar viscosity)= 0.00002143 kg/m-s (air)
DEN(density)= 0.9611 kg/m

Hence,
Λ (compressibility number)= 6.0
L/D(length to diameter ratio)= 1.0
ϵ (eccentricity ratio)= 0.6
The computed results in terms of dimensionless load capacity, friction coefficient and attitude angle are compared with the data given by Wu [11] using the Reynolds equation approach, namely, isothermal flow without the effects of inertia and turbulence.

	3DNSBRGJ		Reynolds Eqn. Approach
	Isothermal	Non-isothermal	
$\overline{W}$	1.137	1.157	1.028
ϕ	12.8	13.2	19.5
η	3.93 (on bearing) 3.45 (on shaft)	5.96 (on bearing) 4.68 (on shaft)	3.9

The comparison is made for laminar flow. The load capacity obtained by the Navier-Stokes approach is higher than that obtained by the Reynolds equation solution. The non-isothermal case carries higher load than the isothermal case. The fluid inertia enhances the load capacity, and also increases the friction slightly. On the other hand, the temperature rise causes the increase of viscosity of gas, and contributes to the increase of load capacity. However, the temperature change also increases the friction considerably.

To simulate a foil journal bearing, we consider a full journal bearing with a single foil leaf, combination of the top and the bottom foils, which is similar to a MTI's bearing. The foil deforms under the influence of the hydrodynamic pressure and the heat transfer resulted from temperature variation. The foil is given an allowable maximum sway displacement, SWYMX= 0.00005 meter; the rest of data remain the same as the previous example. The variations of load capacity and friction coefficient are then observed.

The comparison of the solid-walled bearing with the foil bearing is tabulated in the followint:

		Solid-Walled Bearing	Foil Bearing
$\overline{W}$	Isothermal	1.137	1.303
	Non-isothermal	1.157	1.323
ϕ	Isothermal	12.8	12.0
	Non-isothermal	13.2	12.2
η	Isothermal	3.93 (on bearing) 3.45 (on shaft)	2.43 (on bearing) 2.48 (on shaft)
	Non-isothermal	5.96 (on bearing) 4.68 (on shaft)	7.48 (on bearing) 3.29 (on shaft)

The deformation of the foil cause the slight increase of load capacity. The drop of friction in the isothermal case is due to the widening of the film gap. For the non-isothermal case, the local thermo-elastic deformation of the foil may create pockets. Consequently, the friction coefficient changes considerably.

For the case of the turbulent flow in the journal bearing, the data of the previous example are modified to have:

RPM= 52000
RS= 0.0508 m
RB= 0.0509336 m
HC= 0.00013363 m
EE= 0.00008018 m
ALEN= 0.1016 m

The L/D ratio and the eccentricity ration remain the same. The Reynolds number increases to be 1658. The bearing compressibility number becomes 1. Results comparing with the Reynolds solution are tabulated in the following:

	3DNSBRGJ solid wall	3DNSBRGJ foil	REYNOLDS SOL. solid wall
$\bar{W}$	0.409	0.490	0.30
η	4.98 (on shaft)	3.31 (on shaft)	2.5 (on shaft)

The decrease of friction for the foil bearing may due to the increase of the film gap.

(B) Thrust Bearing

We consider a thrust bearing with the following input data:

RPM= 35000
PAMB= 101353 N(newton)/sq.m
R1= 0.1 m
R2= 0.2 m
BETA= 0.667 rad.
H1= 0.00016703 m
H2= 0.000012527 m
AMULAN (viscosity)= 2.143E-5 kg/m-sec
DEN(density)=0.961 kg/cube m

The bearing compressibility number Λ, L/B and H1/H2 are calculated as:

$$\Lambda = \frac{6\mu(0.5)(R_1+R_2)\omega B}{P_a (H_2)^2} = 10$$

$$\frac{L}{B} = \frac{0.5(R_1+R_2)\beta}{(R_2-R_1)} = 1$$

$$\frac{H_1}{H_2} = \frac{H_1}{H_2} = 2$$

The computed results for the isothermal case are compared with the Reynolds equation solution for a sector thrust bearing given in [15] and [10]. The results in terms of load capacity and friction coefficient are tabulated in the following:

	3DNSBRGT		REYNOLDS EQUATION SOL.
	Solid-Wall	Foil	
$\bar{W}$	0.0467	0.0514	0.0355
$\bar{F}$	2.98	2.43	0.711

The dimensionless load capacity by the Navier-Stokes solution is higher than that by the Reynolds equation solution. The reason is that the bearing speed is high and the inertial acceleration is significant. The friction force is obtained by selecting 3-point velocity gradient near the wall for the shear stress and integrating over the bearing surface. The great difference of friction coefficient may be partially due to the coarse grid in the numerical computation. However, the increase of friction force by the N-S approach is physically sound. With the deflection of the foil, the load capacity increases and the friction coefficient decreases slightly.

REFERENCE

[1] Constantinescu, V.N., "Analysis of Bearings Operating in Turbulent Regime," ASME Journal of Basic Engineering, Vol.84, 1962, p. 139.

[2] Ng, C.W. and Pan, C.H.T., "A Linearized Turbulent Lubrication Theory," ASME Journal of Basic Engeering, Vol. 87, 1965, p.675.

[3] Elrod, H.G. and Ng, C.W., "A Theory for Turbulent Fluid Films and its Application to Bearings," ASME Journal of Lubrication Technology, Vol. 89, 1967, p.346.

[4] Launder, B.E. and Leschziner, M.A., "Flow in Finite-Width Thrust Bearings Including Inertial Effects, II-Turbulent Flow," ASME Journal of Lubrication Technology, Vol. 100, 1978, p.339.

[5] Jones, W.P. and Launder, B.E., "The Calculation of Low-Reynolds Number Phenomena with a Two Equation Model of Turbulence," Int. J. Heat and Mass Transfer, Vol. 16, 1973, p.1189.

[6] Chen, H.C. and Patel, V.C., "Near-Wall Turbulence Models for Complex Flows Including Separation," AIAA Journal Vol. 26, No. 6, 1988, p. 641.

[7] Martinuzzi, R. and Pollard, A., "Comparative Study of Turbulence Models in Predicting Turbulent Pipe Flow, Part I: Algebraic Stress and K-e Models," AIAA Journal, Vol. 27, No. 1, 1989, p.29.

[8] Patankar, S.V. and Spalding, D.B., "A Calculation Procedure for Heat, Mass and Momentum Transfer in Three Dimensional Parabolic Flows," Int. J. Heat and Mass Transfer, Vol. 15, 1972, p.1787.

[9] Patankar, S.V., Numerical Heat Transfer and Fluid Flow, Hemisphere Publishing Corporation, McGraw-Hill Book Company, 1980.

[10] Pinkus, O. and Sternlicht, B., Theory of Hydrodynamic Lubrication, McGraw-Hill Book Company, 1961.

[11] Wu, E.R., "Gas-Lubricated Porous Bearings of Finite Length--- Self-Acting Journal Bearings," ASME Trans., Journal of Lubrication Technology, Sept., 1979, p.338.

[12] Parkus, H., Thermoelasticity, Blaisdell Publishing Company, Waltham, Massachusetts, 1968.

[13] Walowit, J.A. and Anno, J.N., Modern Developments in Lubrication Mechanics, John Wiley and Sons, 1975.

[14] Heshmat, H., Walowit, J.A. and Pinkus, O., "Analysis of Gas-Lubricated Compliant Thrust Bearings," ASME, Journal of Lubrication Technology, Paper No. 82-Lub-39.

[15] Constantinescu, V.N., Gas Lubrication, The American Society of Mechanical Engineers, 1969.

PROGRAM

Two computer codes, 3DNSBRGJ and 3DNSBRGT, are developed. The names stand for three (3) Dimensional Navier-Stokes Bearing, Journal bearing and Thrust bearing programs. As discussed previously, the geometrical configurations of the two bearings, the journal bearing and the thrust bearing, are different. The coordinate transformations are different. The final forms of the equations are not the same for the two bearings. Hence, it is more efficient to perform the calculations in separate codes than in a single general code. Nevertheless, both codes have the same structure which consists of subroutines performing designated functions:

Subroutine	Function
DATAIN	accepts input data
INITIAL	defines initial conditions
UPSTREM	establishes upstream conditions
VISCOS & GAMA	calculate the effective viscosity coefficients
FILMTK	determines film thickness
FLUX	calculates fluxes
BOUNDRY	set up boundary conditions
SOURCE	calculates source terms
COEFFSL	calculates transport and pressure correction equations
EWPNS	calculates coefficients of algebraic eqns.
COEFMOD	modifies coefficients in algebraic eqns.
SOLVE	solver for algebraic eqns., using both block tri-diagonal matrix and Gauss-Seidel plus over-relaxation interation
WLOAD	calculates performance charateristics
ELASTHM	performs thermoelasticity calculations
CHECK & CHECKA	print out value of variable arrays such as density, viscosity, velocity components, pressure and temperature.

The MAIN program controls the step-by-step marching process. It also writes the results of the current iteration on a disk file and use this disk data as the initial data for the next iteration. In addition, it writes data on disk files for later calculations of bearing performnace charateristics such as load capacity, frictional force and dimensionless parameters.

The program reads input data in the format of NAMELIST. In the following all NAMELISTs for the journal bearing and the thrust bearing will be explained respectively:

(I) Journal Bearing

NAMELIST	VARIABLE	MEANING
BRGDAT	RPM	rpm of shaft
	PAMB	ambient pressure
	RS	radius of shaft
	RB	radius of bearing bore
	BETA	subtended angle of foil
	BETAS	starting arc angle of foil
	BETA1	ending arc angle of fluid film on foil
	HC	radial clearance
	EE	eccentric displacement of shaft
	ALEN	length of shaft
FLUIDAT	AMULAM	laminar flow viscosity
	PRLAM	laminar flow Prandtl number
	DEN	initial fluid density
	CP	heat capacity at constant prssure
	CPDCV	ratio of Cp to Cv
	GASCON	gas constant of fluid
	PR	Prandtl numbers for all dependent variables

	AKFAC	turbulent flow constant for initial condition (4.3E-6)
	WM	molecular weight of fluid
	PIN	initial pressure
	TIN	initial temperature
	PCRIT	pressure correction equation criterion (2.0)
GRIDAT	A1,A2,A3	3 divisions of computation domain in θ direction e.g. 0.25,0.5,0.25
	B1,B2,B3	same as A1,A2,A3 but in z direction. e.g. 0.3333,0.3333, 0.3333
	N1,N2,N3	number of grid points in A1,A2,A3 divisions respectively
	M1,M2,M3	number of grid points in B1,B2,B3 divisions respectively
VOLDAT	L,M	number of control volumes in z & r directions
	IMAX,JMAX	total grid points in z and r directions; IMAX=L+1, JMAX=M+1
	PFAC	relaxation factor on pressure correction (0.95)
	IPF	initial pressure profile selector 0 for sin & cos profile 1 for sin profile only
	PFA,PFB	initial pressure profile amplitude
	FMEG	over-relaxation factor for all dependen variables(1.5-1.8)
CONTL	NSWP	tri-diagonal block matrix solver sweep number for each variable (8*2)
	IXY,ISWP,JSWP	tri-diagonal block matrix sweep index (1,1,1)

	ISOLV	on and off key for solving the transport eqn. for each dependent variable; 1 solve the eqn. C by pass dependent variables are in the order of Vr(1),Vz(2),V_θ(3),p'(4) HH(total enthalpy)(5), k(6),e(7) T(8)
	NNV	total number of dependent variable, NNV=8
	NITER	total number of momentum eqn. iteration
	NELS	total number of thermoelasticity eqn. iteration
	REYCRT	critical Reynolds number
ELSCON	ALPHA	thermal expansion coefficient of foil material
	PATHON	Poisson's ratio of foil material
	YN	Young's modulus of foil material
	T1	top foil thickness
	T2	bottom foil thickness
	WAVL	half wave length of bump(bottom) foil
	SWYMX	maximun displacement of foil sway

(II) Thrust Bearing

BRGDAT	RPM	rpm of shaft
	PAMB	ambient pressure
	R1	inner radius of disk
	R2	outer radius of disk
	BETA	subtended pad angle
	BETA1	subtended fluid film angle
	H1	maximum film gap
	H2	minimum film gap
	HMEAN	mean film gap

FLUIDAT	AMULAM	laminar flow viscosity
	PRLAM	laminar flow Prandtl number
	DEN	initial density of fluid
	CP	heat capacity at constant pressure
	CPDCV	heat capacity ratio of Cp to Cv
	GASCON	gas constant of fluid
	PR	array of Prandtl numbers for all dependent variables
	AKFAC	same as journal bearing
	WM	same as journal bearing
	PIN	same as journal bearing
	TIN	same as journal bearing
	PCRIT	same as journal bearing
GRIDAT	A1,A2,A3	same as journal bearing
	B1,B2,B3	same as journal bearing but in r-direction
	N1,N2,N3	same as journal bearing
	M1,M2,M3	same as journal bearing
VOLDAT	L,M	number of control volumes in r and z directions
	IMAX,JMAX	total grid points in r and z directions
	PFAC	same as journal bearing
	IPF	same as journal bearing
	PFA,PFB	same as journal bearing
CONTL	NSWP	same as journal bearing
	IXY,ISWP,JSWP	same as journal bearing
	ISOLV(8)	same as journal bearing
	NITER,NELS	same as journal bearing
	REYCRT	same as journal bearing
ELSCON	ALPHA	same as journal bearing
	PATHON,YN	same as journal bearing
	T1,T2	top and bottom foil thicknesses

Typical input files for both the journal and the thrust bearings are provided in the following:

(I) Journal Bearing Input Data File:

```
 $BRGDAT RPM=52000.0,PAMB=101352.97,RS=5.08E-2,RB=5.093363E-2,BETA=6.2832,
  BETAS= 0.0,BETA1=6.2832,HC=1.3363E-4,EE=8.0178E-5,ALEN=1.016E-1, $END
 $FLUIDAT AMULAM=2.143E-5,PRLAM=0.7,DEN=0.9611,CP=1009.0,CPDCV=1.4,
  GASCON=8.314E+3,PR(1)=1.0,1.0,1.0,1.0,0.9,1.0,1.3,0.9,0.9,AKFAC=4.3E-7,
  WM=28.93,PIN=101352.97,TIN=367,PCRIT=2.0, $END
 $GRIDAT A1=0.25,A2=0.5,A3=0.25,B1=0.3333,B2=0.3333,B3=0.3333,N1=7,
  N2=10,N3=7,M1=4,M2=5,M3=4, $END
 $VOLDAT L=10,M=10,IMAX=11,JMAX=11,PFAC=0.75,IPF=0,PFA=0.55,PFB=0.55,
  FMEG=1.0, $END
 $CONTL NSWP(1)=2,7*2,IXY=1,ISWP=1,JSWP=1,ISOLV(1)=4*1,3*0,0,NNV=8,
  NITER=1,NELS=2,REYCRT=1000.0, $END
 $ELSCON ALPHA=3.3333E-6,PATHON=0.4091,YN=2.1374E+11,T1=0.0001524,
  T2=0.0001016,WAVL=0.005,SWYMX=5.0E-5, $END
```

(II) Thrust Bearing Input Data File:

```
 $BRGDAT RPM=35000.0,PAMB=101352.97,R1=0.1,R2=0.2,BETA=0.667,
  BETA1= 0.667,H1=0.00016703,H2=8.3515E-5,HMEAN=1.2527E-4, $END
 $FLUIDAT AMULAM=2.143E-5,PRLAM=0.7,DEN=0.9611,CP=1009.0,CPDCV=1.4,
  GASCON=8.314E+3,PR(1)=1.0,1.0,1.0,1.0,0.9,1.0,1.3,0.9,0.9,AKFAC=4.3E-8,
  WM=28.93,PIN=101352.97,TIN=367,PCRIT=2.0, $END
 $GRIDAT A1=0.25,A2=0.5,A3=0.25,B1=0.3333,B2=0.3333,B3=0.3333,N1=7,
  N2=10,N3=7,M1=4,M2=5,M3=4, $END
 $VOLDAT L=10,M=6,IMAX=11,JMAX=7,PFAC=0.99,IPF=0,PFA=0.25,PFB=0.35, $END
 $CONTL NSWP(1)=2,7*2,IXY=1,ISWP=1,JSWP=1,ISOLV(1)=4*1,3*0,0,NNV=8,
  NITER=1,NELS=2,REYCRT=5000.0, $END
 $ELSCON ALPHA=3.333E-6,PATHON=0.4091,SWYMX=1.E-5,YN=2.1374E+11,
  T1=0.0001524, T2=0.0001016, $END
```

CONCLUSION

The successful completion of this Phase I study has presented an advanced analytical tool for predicting the performance of foil bearings and solid-walled bearings as well, operating at speeds wherein the Reynolds number is no longer small and the effects of the fluid inertia, the heat transfer and the turbulent flow become significant. The tool utilizes the three dimensional Navier-Stokes approach for the fluid film thermohydrodynamics and the thermoelasticity treatment for the foil deformation.

The Navier-Stokes approach is much more complicated than the Reynolds equation approch, conventional or modified for the inclusion of inertia or turbulence. Nevertheless, the N-S approach has the capability of investigating the local behaviors of the lubricant and the foil. Especially, the prediction of the temperature variation may eventually help explain the hot spots or burned spots which are often observed in a failed bearing.

Naturally, to shed light on the success or the failure of a bearing design, the steady-state solution even as complex as the Navier-Stokes approach, is just the first step. Further studies should include the transient case, the combined bearing-rotor dynamics and possibly an expert system for optimizing the design process.

The accomplishment of the present study has established a foundation for pursuing the just mentioned further steps. The formulations, the coordinate transformations and the numerical solution algorithm can be extended to deal with the transient case and to incorporate with the rotor dynamic analysis.

Two computer programs, 3DNSBRGJ (for the journal bearing) and 3DNSBRGT (for the thrust bearing) are developed through this Phase I study. These programs are capable for predicting the bearing performance characteristics and calculating the velocity components, the temperature distribution, the foil deflection, the turbulence energy distribution and its dissipation rate.

*U.S.Government Printing Office: 1989 — 748-056/24119